

See discussions, stats, and author profiles for this publication at: <https://www.researchgate.net/publication/26877630>

# Phase Transition in Salt-Free Catanionic Surfactant Mixtures Induced by Temperature

ARTICLE *in* LANGMUIR · OCTOBER 2009

Impact Factor: 4.46 · DOI: 10.1021/la902069w · Source: PubMed

CITATIONS

22

READS

21

10 AUTHORS, INCLUDING:



Xia Xin

Shandong University

59 PUBLICATIONS 539 CITATIONS

SEE PROFILE



Tomasz Kalwarczyk

Instytut Chemii Fizycznej PAN

26 PUBLICATIONS 261 CITATIONS

SEE PROFILE



Tomasz Szyborski

Instytut Chemii Fizycznej PAN

13 PUBLICATIONS 128 CITATIONS

SEE PROFILE



Damian Pocięcha

University of Warsaw

190 PUBLICATIONS 2,446 CITATIONS

SEE PROFILE

## Phase Transition in Salt-Free Catanionic Surfactant Mixtures Induced by Temperature

Hongguang Li,<sup>†</sup> Stefan A. Wieczorek,<sup>†</sup> Xia Xin,<sup>†</sup> Tomasz Kalwarczyk,<sup>†</sup> Natalia Ziebaczyk,<sup>†</sup> Tomasz Szymborski,<sup>†</sup> Robert Hołyst,<sup>\*,†,‡</sup> Jingcheng Hao,<sup>\*,§</sup> Ewa Gorecka,<sup>||</sup> and Damian Pocięcha<sup>||</sup>

<sup>†</sup>Department III, Institute of Physical Chemistry, Polish Academy of Sciences, Kasprzaka 44/52, 01-224 Warsaw, Poland, <sup>‡</sup>Department of Mathematics and Natural Sciences, College of Science, Cardinal Stefan Wyszyński University, Dewajtis 5, 01-815 Warsaw, Poland, <sup>§</sup>Key Laboratory of Colloid and Interface Chemistry, Shandong University, Ministry of Education, Jinan 250100, PR China, and <sup>||</sup>Department of Chemistry, University of Warsaw, Al. Zwirki i Wigury 101, Warsaw, Poland

Received June 9, 2009. Revised Manuscript Received September 15, 2009

Aggregate transitions in salt-free catanionic surfactant mixtures of tetradecyltrimethylammonium hydroxide (TTAOH)/fatty acid were investigated as a function of surfactant concentration and temperature. Lauric acid (LA), myristic acid (MA), and palmitic acid (PA) were chosen for the current study. The TTAOH/LA mixture exhibited rich phase behavior at room temperature. With increasing total surfactant concentration ( $c_T$ ), a bluish vesicular ( $L_{av}$ ) phase, an isotropic micellar ( $L_1$ ) phase, and a birefringent lamellar ( $L_\alpha$ ) phase were observed. Between the  $L_{av}$  phase and the  $L_1$  phase, a narrow  $L_\alpha'/L_1$  two-phase region was determined. With increasing temperature, a transition from the  $L_\alpha$  phase to the  $L_1$  phase was induced at higher  $c_T$  whereas at lower  $c_T$  an opposite transition from the  $L_1$  phase to the  $L_{av}$  phase was noticed. Thus surprisingly, we observed bilayer-to-micelle and micelle-to-bilayer transitions in the same catanionic surfactant system, both induced by the temperature increase. Replacing LA by MA and PA caused a continuous increase in the average Krafft point of the mixture. The  $L_{av}$ -phase region and phase-separated region become larger. Moreover, a single  $L_1$ -phase region was absent within the investigated temperature range.

### Introduction

Surfactant molecules can self-assemble in water into a variety of aggregates, including micelles, vesicles, and lyotropic liquid crystals. These molecular assemblies are not only of great fundamental interest but also have attractive potential applications. During the past few decades, considerable attention has been paid to the formation of molecular assemblies and phase transitions in cationic/anionic (catanionic) surfactant mixtures.<sup>1–9</sup> Because of electrostatic interactions between oppositely charged surfactant headgroups, cationic and anionic surfactants tend to form ion pairs when they are mixed in water. This phenomenon leads to an effective reduction of the area of surfactant headgroups and imparts extremely high surface activity to the ion pair. The surfactant ion pair behaves as a double-tailed amphiphile and tends to form molecular bilayers. Thus, vesicles can spontaneously form in catanionic mixtures in dilute aqueous

solutions.<sup>2,10,11</sup> However, when the mixing molar ratio approaches 1 a precipitate will usually form as a result of the screening of the electrostatic interaction between oppositely charged surfactant groups by small counterions.<sup>12</sup> This is a big obstacle to further study and potential applications of catanionic surfactant mixtures. To solve this problem, different methods including extraction and dialysis have been proposed to eliminate the small counterions.<sup>13–16</sup> In recent years, so-called salt-free catanionic surfactant systems have been prepared by mixing alkyl-trimethylammonium hydroxide with fatty acids in water.<sup>12,17–25</sup> In this case, small counterions can be partially eliminated (at a nonequimolar mixing ratio) or totally (at an equimolar mixing ratio) and the system exhibits diverse aggregate transitions upon changing the mixing ratio and total surfactant concentration.<sup>25</sup> Bicompatible salt-free catanionic surfactant mixtures

\*Authors to whom correspondence should be addressed. E-mail: holeyst@ptys.ichf.edu.pl; jhao@sdu.edu.cn.

(1) Kaler, E. W.; Herrington, K. L.; Murthy, A. K.; Zasadzinski, J. A. N. *Science* **1989**, *245*, 1371.

(2) Kaler, E. W.; Herrington, K. L.; Murthy, A. K. *J. Phys. Chem.* **1992**, *96*, 6698.

(3) Herrington, K. L.; Kaler, E. W.; Miller, D. D.; Zasadzinski, J. A.; Chiruvolu, S. *J. Phys. Chem.* **1993**, *97*, 13792.

(4) Yattilla, M. T.; Herrington, K. L.; Brasher, L. L.; Kaler, E. W.; Chiruvolu, S.; Zasadzinski, J. A. *J. Phys. Chem.* **1996**, *100*, 5874.

(5) Iampietro, D.; Kaler, E. W. *Langmuir* **1999**, *15*, 8590.

(6) Koehler, R. D.; Raghavan, S. R.; Kaler, E. W. *J. Phys. Chem. B* **2000**, *104*, 11035.

(7) Raghavan, S. R.; Fritz, G.; Kaler, E. W. *Langmuir* **2002**, *18*, 3797.

(8) Schubert, B. A.; Kaler, E. W.; Wagner, N. J. *Langmuir* **2003**, *19*, 4079.

(9) González, Y. I.; Stjern Dahl, M.; Danino, D.; Kaler, E. W. *Langmuir* **2004**, *20*, 7053.

(10) Safran, S. A.; Pincus, P.; Andelman, D. *Science* **1990**, *248*, 354.

(11) Schmolzer, St.; Gräbner, D.; Gradziński, M.; Narayanan, T. *Phys. Rev. Lett.* **2002**, *88*, 258301–1.

(12) Horbaschek, K.; Hoffmann, H.; Hao, J. *J. Phys. Chem. B* **2000**, *104*, 2781.

(13) Jokela, P.; Jönsson, B.; Khan, A. *J. Phys. Chem.* **1987**, *91*, 3291.

(14) Fukuda, H.; Kawata, K.; Okuda, H. *J. Am. Chem. Soc.* **1990**, *112*, 1635.

(15) Hassan, P. A.; Valaulikar, B. S.; Manohar, C.; Kern, F.; Bourdieu, L.; Candau, S. J. *Langmuir* **1996**, *12*, 4350.

(16) Narayanan, J.; Manohar, C.; Kern, F.; Lequeux, F.; Candau, S. L. *Langmuir* **1997**, *13*, 5235.

(17) Horbaschek, K.; Hoffmann, H.; Thunig, C. *J. Colloid Interface Sci.* **1998**, *206*, 439.

(18) Hao, J.; Liu, W.; Xu, G.; Zheng, L. *Langmuir* **2003**, *19*, 10635.

(19) Song, A.; Dong, S.; Jia, X.; Hao, J.; Liu, W.; Liu, T. *Angew. Chem., Int. Ed.* **2005**, *44*, 4018.

(20) Shen, Y.; Hao, J.; Hoffmann, H. *Soft Matter* **2007**, *3*, 1407.

(21) Zemb, Th.; Dubois, M.; Demé, B.; Gulik-Krzywicki, Th. *Science* **1999**, *283*, 816.

(22) Dubois, M.; Demé, B.; Gulik-Krzywicki, Th.; Dedieu, J.-C.; Vautrin, C.; Désert, S.; Perez, E.; Zemb, Th. *Nature* **2001**, *411*, 672.

(23) Meister, A.; Dubois, M.; Belloni, L.; Zemb, Th. *Langmuir* **2003**, *19*, 7259.

(24) Dubois, M.; Lizunov, V.; Meister, A.; Gulik-Krzywicki, Th.; Verbavatz, J. M.; Perez, E.; Zimmerberg, J.; Zemb, Th. *Proc. Natl. Acad. Sci. U.S.A.* **2004**, *101*, 15082.

(25) Li, H.; Hao, J. *J. Phys. Chem. B* **2008**, *112*, 10497.

made from choline cations and fatty acids have also been prepared.<sup>26,27</sup>

Of particular interest is the aggregate transitions induced by temperature in catanionic surfactant mixtures. Salt-free equimolar mixtures of cationic and anionic surfactants exhibit some peculiar properties in the solid state.<sup>28–30</sup> In bulk aqueous solutions, a vesicle-to-micelle transition induced by increasing temperature has been observed in the system of cetyltrimethylammonium hydroxynaphthalenecarboxylate (CTAHNC).<sup>31–34</sup> and hexadecyltrimethylammonium octylsulfonate (TASO).<sup>35</sup> In some catanionic surfactant mixtures where small counterions are still present, an opposite transition from micelles to vesicles has also been observed with increasing temperature.<sup>36,37</sup> Generally speaking, transitions between micelles and vesicles are governed by the curvature change of a surfactant monolayer or bilayer, which is further controlled by the surface charge density in the case of ionic surfactants. Although several examples of vesicle-to-micelle transition have been observed in catanionic surfactant systems with temperature rising, the dominating factors behind them vary from system to system. Thus, different explanations are usually given by different authors to explain similar phenomena in different systems. For example, Manohar et al. gave a mechanism for a Coulombic solid–fluid transition on a micellar surface to explain the vesicle-to-micelle transition in the cetyltrimethylammonium hydroxynaphthalenecarboxylate (CTAHNC)<sup>31–33</sup> system, and Marques et al. explained the vesicle-to-micelle transition by the dissociation of the octylsulfonate anion into bulk solution at higher temperature, which is believed to have a higher solubility in water compared to that of the hexadecyltrimethylammonium cation.<sup>35</sup> In cases of micelle-to-vesicle transition induced by temperature, the mechanism is still claimed to be unclear.<sup>36,37</sup> Taking into account these considerations, more work is needed to further clarify these interesting aggregate transitions induced by temperature in catanionic surfactant mixtures.

Recently, we have described the phase behavior of a salt-free catanionic surfactant system, tetradecyltrimethylammonium hydroxide (TTAOH)/lauric acid (LA)/H<sub>2</sub>O.<sup>25</sup> At an equimolar mixing ratio of TTAOH and LA, a vesicular (L<sub>av</sub>) phase forms that does not undergo an obvious transition with increasing temperature. This is quite different from the other salt-free catanionic surfactant systems with equimolar mixing ratios studied by Manohar et al. and Marques et al., which undergo a vesicle-to-micelle transition with increasing temperature.<sup>31–35</sup> A question arises as to whether aggregate transitions between micelles and bilayer structures can exist in this type of system. Here we show that by a suitable adjustment of the mixing molar ratio of LA to TTAOH ( $\rho = n_{\text{LA}}/n_{\text{TTAOH}} = 0.88$ ) two distinct

transitions (i.e., lamella to micelle and micelle to vesicle) can be induced by increasing temperature. The transitions strongly depend on the total surfactant concentration ( $c_{\text{T}} = c_{\text{TTAOH}} + c_{\text{LA}}$ ). The presence of vesicles and lamellae have been clearly identified by fluorescence microscopy observations and small-angle X-ray scattering (SAXS) measurements, respectively, and the lamella-to-micelle transition process was monitored by polarized microscopy observations. We also show that these phase transitions are influenced by the surfactant chain length, characterized by different fatty acids herein from lauric acid (LA) to myristic acid (MA) and palmitic acid (PA).

## Experimental Section

**Chemicals and Materials.** Lauric acid (LA), myristic acid (MA), and palmitic acid (PA) with purities of >98% were purchased from Fluka and used without further purification. TTAOH stock solution was prepared following the procedures described previously.<sup>25</sup> Fluorescein was purchased from Riedel de Haen and used as received.

**Preparation of TTAOH/Fatty Acid Mixtures.** To three glass bottles each containing 100 mL of TTAOH stock solution the desired amounts of solid LA, MA, and PA were added. The mixing molar ratio of each fatty acid to TTAOH was fixed at 0.88. The samples were then kept at 50 °C in an oven to allow the acid–base reactions to occur, during which time frequent hand-shaking was performed. After all of the solid fatty acids were dissolved, the samples were kept in the oven for 1 more week to ensure the completion of the acid–base reactions. Afterwards, the samples were dried at 40 °C in the oven and the solid was collected for further use.

**Phase Behavior Study.** The phase behavior was recorded by visual inspection and crossed polarizers. The temperature, which was controlled with a water bath or an oven, was increased from 25 to 60 °C in increments of 5 °C. At each temperature, the samples were gently hand-shaken to get homogeneous solutions at the starting point and were then left to equilibrate for 2 weeks.

**Fluorescence Microscopy Observations.** Fluorescence microscopy observations were carried out on a Nikon Eclipse 50i microscope equipped with a black and white fluorescence camera. The samples were labeled with fluorescein at a final concentration of  $\sim 10^{-5}$  M. A filter was used that can cut off excited light below 465 nm and above 495 nm.

**SAXS Measurements.** SAXS measurements were carried out using Cu K $\alpha$  radiation of 0.15418 nm with a Bruker Nanostar system and a Vantec 2000 area detector. Samples were prepared by filling thin glass capillaries of 1.5 or 2.0 mm diameter, which were then flame-sealed immediately. The signal intensities were obtained through integration of the 2D patterns over the azimuthal angle. The temperature was changed from 23 to 30, 35, and 40 °C, respectively. For the sample with  $\rho = 0.91$ , SAXS measurement were carried out on the beamline 4B9A synchrotron radiation X-ray small-angle system at the Beijing Synchrotron Radiation Facility.

**Polarized Microscopy Observations.** Polarized microscopy observations were carried out on a Nikon Eclipse E400 microscope with a crossed polarizer equipped with a Linkam THMS 600 heating/cooling stage. The stage was controlled by a computer program called LinkSys 2.36 with temperature control of  $\pm 0.01$  °C. The temperature was increased from 25 to 60 °C in increments of 5 °C. Samples were prepared between two circular glasses whose edges were immediately sealed with epoxy resin glue. The thickness of the sample was about 2 mm. We carried out observations both immediately after sample preparation and 2 days later to check the influence of the shear force introduced during sample preparation. Although the shear force was found to have some influence on the static texture of the L <sub>$\alpha$</sub>  phase,<sup>25</sup> it did not have an obvious influence on the temperature-induced texture evolution during the L <sub>$\alpha$</sub>  to L<sub>1</sub> phase transition.

(26) Klein, R.; Touraud, D.; Kunz, W. *Green Chem.* **2008**, *10*, 433.

(27) Klein, R.; Kellermeier, M.; Drechsler, M.; Touraud, D.; Kunz, W. *Colloids Surf., A* **2009**, *338*, 129.

(28) Filipović-Vinceković, N.; Pucić, I.; Popović, S.; Tomašić, V.; Težak, Đ. *J. Colloid Interface Sci.* **1997**, *188*, 396.

(29) Tomašić, V.; Popović, S.; Filipović-Vinceković, N. *J. Colloid Interface Sci.* **1999**, *215*, 280.

(30) Silva, B. F. B.; Marques, E. F. *J. Colloid Interface Sci.* **2005**, *290*, 267.

(31) Salkar, R. A.; Hassan, P. A.; Samant, S. D.; Valaulikar, B. S.; Kumar, V. V.; Kern, F.; Candau, S. J.; Manohar, C. *Chem. Commun.* **1996**, 1223.

(32) Hassan, P. A.; Valaulikar, B. S.; Manohar, C.; Kern, F.; Bourdieu, L.; Candau, S. J. *Langmuir* **1996**, *12*, 4350.

(33) Menon, S. V. G.; Manohar, C.; Lequeux, F. *Chem. Phys. Lett.* **1996**, *263*, 727.

(34) Horbaschek, K.; Hoffmann, H.; Thunig, C. *J. Colloid Interface Sci.* **1998**, *206*, 439.

(35) Silva, B. F. B.; Marques, E. F.; Olsson, U. *Langmuir* **2008**, *24*, 10746.

(36) Yin, H.; Zhou, Z.; Huang, J.; Zheng, R.; Zhang, Y. *Angew. Chem., Int. Ed.* **2003**, *42*, 2188.

(37) Yin, H.; Huang, J.; Lin, Y.; Zhang, Y.; Qiu, S.; Ye, J. *J. Phys. Chem. B* **2005**, *109*, 4104.

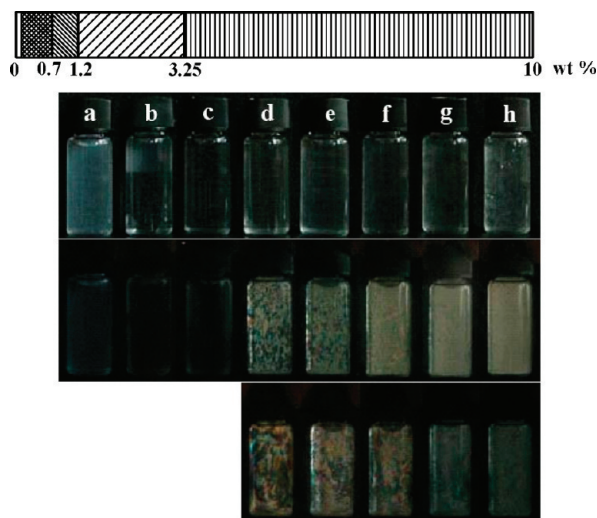


**Figure 1.** (Top) Phase diagram of the TTAOH/LA mixture in water with  $\rho = 0.88$  recorded at room temperature ( $\sim 22^\circ\text{C}$ ). ( $\square$  region near 0 wt %) Phase-separated region; (cross-hatched region from  $> 0$  to 0.7 wt %)  $L_{\alpha v}$  phase; (diagonal lines from 0.7 to 1.2 wt %)  $L_{\alpha'}/L_1$  two-phase region; (diagonal lines from 1.2 to 3.25 wt %)  $L_1$  phase; and (vertical-lined region from 3.25 to 10 wt %)  $L_{\alpha}$  phase. (Bottom) Photographs of typical samples within different phase regions. From a to h,  $c_T$  (wt %) is 0.60, 0.98, 1.97, 3.77, 4.90, 6.06, 7.39, and 9.13, respectively. (First row) Without polarizers; (second row) with crossed polarizers; and (third row) photographs of samples in the  $L_{\alpha}$ -phase region between crossed polarizers after gentle hand-shaking.

## Results and Discussion

**Phase Behavior at Room Temperature.** The phase behavior of the TTAOH/LA mixture in water with  $\rho = 0.88$  at room temperature together with photographs of typical samples within different regions are given in Figure 1. At high dilution ( $c_T < 0.1$  wt %), some white flocculation was observed at the top of the bulk solution, which is nearly transparent. With increasing  $c_T$ , the area of the flocculation region shrinks and the bulk solution begins to be bluish, which is a typical feature of the vesicular ( $L_{\alpha v}$ ) phase. At  $c_T > 0.7$  wt %, the  $L_1$  phase forms at the bottom, and the volume increases continuously with increasing  $c_T$ . At  $c_T > 1.2$  wt %, the turbid upper phase (denoted as  $L_{\alpha'}$ ) disappears and a single  $L_1$ -phase region is reached. The  $L_1$  phase is transparent, optically isotropic, and very viscous. Rheological measurements revealed the presence of wormlike micelles.<sup>25</sup> At higher concentration, flow birefringence was also noticed. When  $c_T$  exceeds 3.25 wt %, a birefringent lamellar ( $L_{\alpha}$ )-phase region is reached, and the birefringence in this region becomes stronger once disturbed by shear (bottom of Figure 1, third row).

Figure 2 gives a typical fluorescence micrograph of large vesicles in the  $L_{\alpha v}$  phase. The vesicles are crowded and poly-disperse, ranging from hundreds of nanometers to several micrometers. In some parts, two or more vesicles can contact each other (solid arrows). For vesicles formed by only one kind of ionic surfactant such as DDAB, the surface charge density of the bilayer is high. For catanionic vesicles, however, the bilayer contains both cationic and anionic components and the surface charge density is lower, making it easier for adjacent vesicles to get close. Together with globular vesicles, some deformed vesicles typically with cylindrical shapes are also noticed (empty arrows). Although FF-TEM and cryo-TEM are powerful techniques for capturing vesicles with submicrometer length scales, the fluorescence microscopy technique has the advantage of capturing vesicles typically with micrometer length scales, thus providing

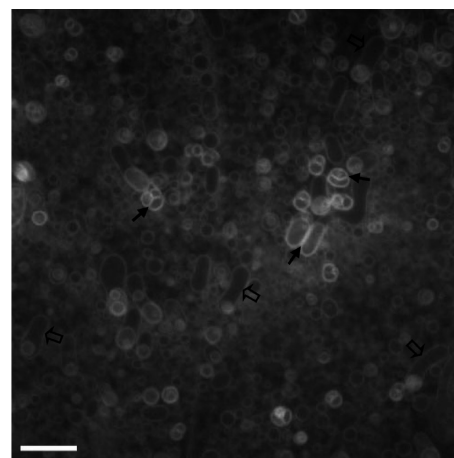


**Figure 2.** Typical fluorescence micrograph of large vesicles formed in the  $L_{\alpha v}$  phase.  $\rho = 0.88$  and  $c_T = 0.4$  wt %. The bar corresponds to 10  $\mu\text{m}$ .

an alternative method for studying catanionic vesicles. Other techniques such optical microscopy<sup>32</sup> or the cryo-SEM technique<sup>35</sup> were used to capture large catanionic vesicles in some catanionic surfactant mixtures. Compared to those techniques, however, the fluorescence microscopy method provides pictures with much higher contrast.

The structural details of the  $L_{\alpha}$  phases were characterized by SAXS measurements, and a typical result recorded for the sample with  $c_T = 9.13$  wt % is given in Figure 3. Three peaks were detected with relative position ratio to be 1:2:3, indicating a lamellar structure. The interlayer spacing  $d$ , calculated from the position of the first peak ( $d = 2\pi/q_{\text{max}}$ ), was 19.5 nm. When  $c_T$  was lowered, a continuous increase in  $d$  was observed. For samples with  $c_T$  values of 6.59 and 4.90 wt %,  $d$  values of 22.7 and 36.0 nm were measured, respectively. The SAXS carried out on a sample with  $\rho = 0.91$  and  $c_T = 3.38$  wt % gave an even larger  $d$  value of 50.8 nm. At lower surfactant concentration, the number of bilayers is smaller than that at higher surfactant concentration, accounting for the swelling of the  $L_{\alpha}$  phase and the increase in  $d$  value with the continuous decreasing in  $c_T$ . When  $c_T$  was lowered, the difficulty in obtaining relative peaks in the lamellar phase increased significantly. This could be ascribed to the decrease in the bilayer number density and more pronounced lamella fluctuation at lower  $c_T$ . Compared with the case at higher  $c_T$  as shown in Figure 3, the peaks obtained at lower  $c_T$  were usually broad and in some cases even bimodal (Supporting Information). The structure of these peaks indicated that some other ordered structures coexisted with the  $L_{\alpha}$  phase close to the  $L_{\alpha}/L_1$  phase boundary. Similar problems were pointed out by other authors.<sup>38–41</sup> For example, Hoffmann et al. pointed out that the  $L_{\alpha}$  phase can coexist with the vesicular or  $L_3$  phase in the alkyltrimethylammonium hydroxide/heptanol/water system,<sup>38</sup> and Dubois et al. found that the lamellar structure can coexist with disklike micelles in the cetyltrimethylammonium hydroxide/myristic acid/water system.<sup>39</sup>

Between the  $L_{\alpha v}$  phase and single  $L_1$  phase an  $L_{\alpha'}/L_1$  two-phase region forms with a turbid  $L_{\alpha'}$  phase at the top. Examinations of the weight percent of surfactants involved in the upper and bottom phases for a sample with  $c_T = 0.8$  wt % indicates that

(38) Hoffmann, H.; Thunig, C.; Munkert, U. *Langmuir* **1992**, *8*, 2629.

(39) Dubois, M.; Carrière, D.; Iyer, R.; Arunagirinathan, M. A.; Bellare, J.; Verbavatz, J.-M.; Zemb, Th. *Colloids Surf, A* **2008**, *319*, 90.

(40) Garstecki, P.; Holyst, R. *Langmuir* **2002**, *18*, 2519.

(41) Garstecki, P.; Holyst, R. *Langmuir* **2002**, *18*, 2529.



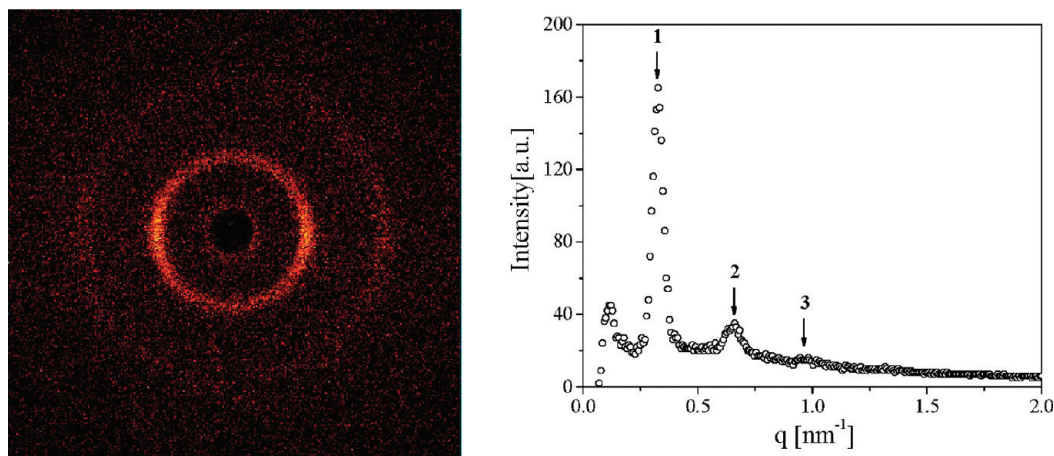


**Figure 3.** (Left) Two-dimensional SAXS diffraction pattern and (right) corresponding scattering peaks after the signal integral for an  $L_{\alpha}$  phase formed by the TTAOH/LA mixture in water with  $\rho = 0.88$  and  $c_T = 9.13$  wt %.

the individual  $c_T$  is 1.661 wt % for the upper phase and 0.363 wt % for the bottom phase; therefore, the upper  $L_{\alpha}'$  phase was much richer in surfactant than the bottom  $L_1$  phase. Fluorescence microscopy observations revealed that in the upper  $L_{\alpha}'$  phase very crowded vesicles were formed. Surprisingly, vesicles have also been detected in the bottom  $L_1$  phase, where the vesicles are larger and more dispersed than in the upper  $L_{\alpha}'$  phase (Supporting Information). In contrast, in the single  $L_1$  phase region no vesicles were found at all. This indicates that the bottom phase within the  $L_{\alpha}'/L_1$  two-phase region is not a real  $L_1$  phase but rather a mixture of micelles and vesicles.

#### Aggregate Transitions Induced by Temperature.

Figure 4A shows the phase behavior as a function of surfactant concentration and temperature for the TTAOH/LA mixture in water with  $\rho = 0.88$ . With increasing temperature, a transition from the  $L_{\alpha}$  phase (lamella) to the  $L_1$  phase (micelle) is induced at higher  $c_T$  whereas at lower  $c_T$  an opposite transition from the  $L_1$  phase (micelle) to the  $L_{\alpha v}$  phase (vesicle) is noticed. To the best of our knowledge, this is the first time that both bilayer-to-micelle and micelle-to-bilayer transitions have occurred in the same catanionic surfactant system induced by a temperature increase. During the lamella-to-micelle transition, the  $L_1$  phase forms from the bottom of the  $L_{\alpha}$  phase and its volume increases gradually with increasing temperature. The higher the  $c_T$  of the  $L_{\alpha}$  phase, the higher the temperature at which the  $L_{\alpha}$  to  $L_1$  phase transition occurs. Thus, the volume fraction of the upper  $L_{\alpha}$  phase increases with increasing  $c_T$  at a fixed temperature and decreases with increasing temperature at a fixed  $c_T$  (Supporting Information).

The transition from micelles to vesicles, which is separated by an  $L_{\alpha}'/L_1$  two-phase region, is not obvious below 45 °C. Above 45 °C, the  $L_{\alpha v}$ -phase region expands to higher  $c_T$  at the expense of the adjacent  $L_{\alpha}'/L_1$  two-phase region. Correspondingly, the  $L_{\alpha}'/L_1$  two-phase region expands to higher  $c_T$  at the expense of the adjacent  $L_1$ -phase region. Even within the  $L_1$ -phase region, which is usually transparent, a small amount of white flocculation formed above 45 °C. It could be easily redispersed by gentle hand-shaking, making the  $L_1$  phase more or less turbid. This clouding phenomenon is probably due to the formation of aggregated large multilamellar vesicles within the  $L_1$  phase with increasing temperature.

Replacing LA by MA and PA causes obvious changes in the phase behavior, as shown in Figure 4B,C. As the chain length of fatty acid increases, both the  $L_{\alpha v}$  phase region and the phase-separated region broaden while the  $L_{\alpha}$ -phase region shrinks. Moreover, for MA and PA, a single  $L_1$ -phase region is missing.

With a longer chain length of fatty acid, a corresponding increase in the average Krafft point is also induced. Whereas the TTAOH/LA mixture has an average Krafft point well below room temperature, the TTAOH/MA and TTAOH/PA mixtures have average Krafft points of around 25 and 33 °C, respectively. The average Krafft point shows a dependence on the surfactant concentration. Similar observations have also been made in mixtures of didodecyldimethylammonium (DDAB) with some anionic surfactants such as sodium dodecylsulfate (SDS)<sup>42–44</sup> or sodium dioctylsulfosuccinate (AOT)<sup>45</sup> and were ascribed to the counterion effect<sup>46</sup> because a change in surfactant concentration is always accompanied by a change in counterion concentration.

Unlike the phase-separated region in the TTAOH/LA mixture that is dominated by an  $L_{\alpha}/L_1$  two-phase region, the phase-separated region in the TTAOH/MA and TTAOH/PA mixtures is dominated by the  $L_{\alpha}'/L_1$  two-phase region where the upper phase is nearly opaque. At higher temperatures, however, the opaque  $L_{\alpha}'$  phase becomes unstable and transforms gradually with time to a transparent  $L_{\alpha}$  phase and a flocculated phase, which is the third condensed phase at the phase boundary. The mechanism behind the  $L_{\alpha}'$ -to- $L_{\alpha}$  phase transition is currently not very clear. It is probably controlled by kinetic factors because of the thermodynamically unstable  $L_{\alpha}'$  phase. In fact, on the basis of previous papers, we could expect pronounced metastability in surfactant systems.<sup>47,48</sup>

**Polarized Microscopy Observation and SAXS Measurements.** Because the  $L_{\alpha}$  phase is birefringent and the  $L_1$  phase is optically isotropic, the lamella-to-micelle transition can be well monitored by temperature-controlled polarized microscopy observations. Typical results carried out on a sample with  $c_T = 5.58$  wt % are given in Figure 5. One can see that the texture of the  $L_{\alpha}$  phase fades with increasing temperature. More observations revealed that texture fading occurs at higher temperature for the sample with a higher  $c_T$  (Supporting Information), which is consistent with the above-mentioned phase-behavior study.

(42) Kondo, Y.; Uchiyama, H.; Yoshino, N.; Nishiyama, K.; Abe, M. *Langmuir* **1995**, *11*, 2380.

(43) Marques, E. F.; Regev, O.; Khan, A.; Miguel, M. G.; Lindman, B. J. *Phys. Chem. B* **1998**, *102*, 6746.

(44) Marques, E. F.; Regev, O.; Khan, A.; Miguel, M. G.; Lindman, B. J. *Phys. Chem. B* **1999**, *103*, 8353.

(45) Caria, A.; Khan, A. *Langmuir* **1996**, *12*, 6282.

(46) Bales, B. L.; Benrraou, M.; Zana, R. *J. Phys. Chem. B* **2002**, *106*, 9033.

(47) Holyst, R.; Staniszewski, K.; Demyanchuk, I. *J. Phys. Chem. B* **2005**, *109*, 4881.

(48) Holyst, R.; Staniszewski, K.; Patkowski, A.; Gapinski, J. *J. Phys. Chem. B* **2005**, *109*, 8533.

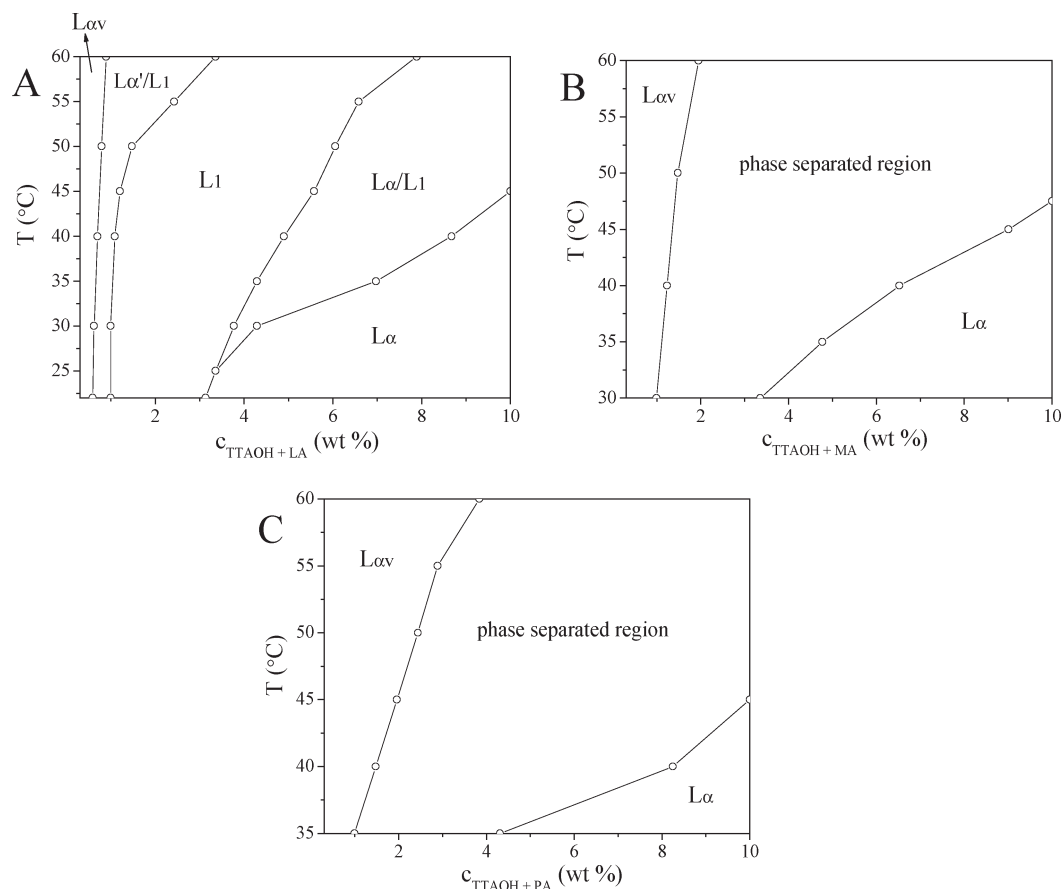


**Figure 4.** Phase diagram of (A) the TTAOH/LA mixture, (B) the TTAOH/MA mixture, and (C) the TTAOH/PA mixture in water as a function of surfactant concentration and temperature. The mixing molar ratio of fatty acid to TTAOH is 0.88 in all cases. We prepared samples in the  $c_T$  range of 0.3–10 wt % in increments of 0.5 wt %. Near the phase-transition boundaries, additional samples were prepared to determine the boundaries more precisely.

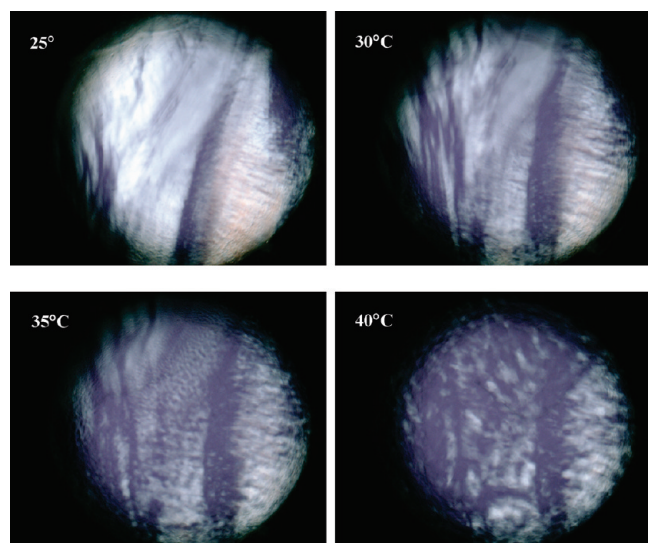


**Figure 5.** Evolution of textures induced by temperature for a typical sample within the  $L_\alpha$  phase region.  $c_T = 5.58$  wt %. Images were obtained from the same region of the sample, and the magnification is the same with a total width of 2.7 mm.

SAXS measurements were carried out at different temperatures for a typical  $L_\alpha$  phase with  $c_T = 9.13$  wt %, and the results are summarized in Figure 6. The highest temperature is 40 °C, which is well below the  $L_\alpha$ -to- $L_1$  phase-transition point for this sample (Figure 4). The temperature-induced swelling of the  $L_\alpha$  phase did

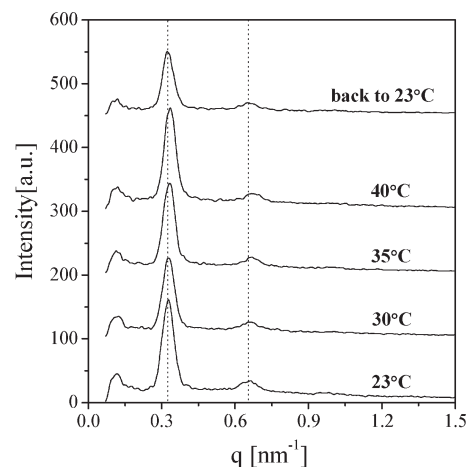


**Figure 6.** SAXS results recorded at different temperatures for a typical  $L_\alpha$  phase with  $c_T = 9.13$  wt %. The intensity for the bottom curve is the real value, and the other curves moved along the  $y$  axis for better clarity. The two straight dotted lines are guides to the eyes.

not occur because  $d$  did not change much within the selected temperature range. Instead, the peak position slightly moved to higher  $q$  values at higher temperatures, indicating a continuous decrease in  $d$  with increasing temperature. For example, the  $d$  value at 23 °C was 19.5 nm and changed gradually to 18.8 nm at 40 °C. When the sample was cooled from 40 °C back to 23 °C,

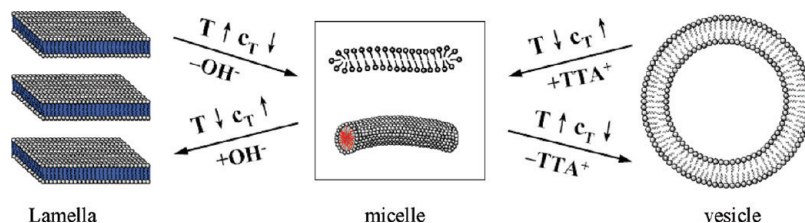


**Figure 7.** Schematic illustration of the aggregate transition between lamella, micelles, and vesicles induced by temperature and surfactant concentration in the TTAOH/LA mixture with TTAOH in slight excess. For simplicity, a rodlike micelle and unilamellar vesicle are shown here. However, wormlike micelles and multilamellar vesicles may also be present.

the peak position and hence  $d$  recovered to the original value. The decrease in  $d$  with increasing temperature can be ascribed to the change in state of the alkyl chains within the surfactant bilayer. Although the alkyl chains are more ordered at room temperature, they will become more and more disordered with increasing temperature. The thickness of the bilayer formed by the disordered alkyl chains is smaller than that formed by the ordered alkyl chains,<sup>49</sup> accounting for the decrease in  $d$  at higher temperatures. When the temperature is changed back to the initial value, the alkyl chains also change from the disordered state back to the ordered state, which leads to a complete recovery of  $d$ .

**Mechanism behind the Lamella-to-Micelle and Micelle-to-Vesicle Transitions.** From the point of view of curvature, the lamella-to-micelle and micelle-to-vesicle transitions proceed in opposite ways; therefore, the mechanisms behind them should be different. In the following text, we will show that the lamella-to-micelle transition may be explained through counterion binding whereas the micelle-to-vesicle transition can be understood by the variation of components involved in the aggregates.

Generally speaking, aggregate transitions in surfactant solutions can be explained by the theory of the critical packing parameter  $p = V/la_0$ , where  $p$  is the critical packing parameter of a given surfactant molecule,  $V$  and  $l$  are the volume and length of the hydrophobic alkyl chain, respectively, and  $a_0$  is the area of the hydrophilic headgroup.<sup>50</sup> The value of  $p$  is closely related to the spontaneous curvature of monolayers or bilayers formed by a given surfactant, which subsequently governs the type of aggregate formed. For an ionic surfactant,  $p$  shows a strong dependence on the electrostatic interactions between surfactant molecules, which is mainly governed by the binding of small counterions. In the case of a catanionic surfactant system such as the TTAOH/LA mixture,  $p$  can be also changed significantly because of the strong association between the two oppositely charged surfactant headgroups, which will cause a significant decrease in  $a_0$ . When the mixing ratio between LA and TTAOH is 1, the surfactant ion pairs can act as a double-tailed surfactant with a  $p$  value of around 1 and can organize themselves into vesicles within a wide  $c_T$  range.<sup>25</sup>

When TTAOH is in excess as in the current case, small counterions of  $\text{OH}^-$  are present. In some cases, lamellar phases form at room temperature ( $c_T > 3.25$  wt % in current case), and the excess  $\text{OH}^-$  should dissociate into bulk water because TTAOH is known as a strong base. Also in studies of double-chained amphiphiles with  $\text{OH}^-$  as counterions,<sup>51–53</sup>  $\text{OH}^-$  was found to have a stronger affinity for water and to sit much further

from a charged surface than chloride or bromide ions. However, we speculate here that some of them may still exist near the lamella and create a negative charge cloud that can lower the surface charge density of the lamella. With increasing temperature, these negative charges begin to move further away, leaving the lamella more positively charged. Driven by the increase in curvature, the transition from lamella to micelle is induced. Because the “dissociation” of the negative charges near the lamella is a continuous process, the lamella-to-micelle transition is also continuous. In some region, lamellas and micelles coexist, forming an  $L_\alpha/L_1$  two-phase region.

The micelle-to-vesicle transition, which occurs at lower  $c_T$ , can be explained by the variation of components involved in the aggregates. The TTAOH/LA mixture with TTAOH in excess is equivalent to a mixed system of a double-tailed surfactant and an excess single-tailed surfactant. The micelles formed in the  $L_1$  phase consist of both surfactant ion pair  $\text{TTA}^+\text{L}^-$  and excess single-tailed surfactant ion  $\text{TTA}^+$ . Because TTAOH has a much higher critical micellar concentration (cmc) than surfactant ion pair  $\text{TTA}^+\text{L}^-$  and the concentration of TTAOH unimers in water can be orders of magnitude higher than that of  $\text{TTA}^+\text{L}^-$ , TTAOH may dissociate gradually into bulk solution with increasing temperature. This will lower the surface charge density and make the micelle transform to aggregates that are not as greatly curved (i.e., vesicle). Similar mechanisms have also been proposed for other systems such as lipid/detergent,<sup>54</sup> lecithin/bile salt,<sup>55</sup> and DDAB/SDS<sup>44</sup> mixtures. At higher temperature, the dissociation of surfactant ion pairs also becomes more obvious ( $\text{TTA}^+\text{L}^- \rightarrow \text{TTA}^+ + \text{L}^-$ ), which can increase the number of free  $\text{TTA}^+$  and facilitate the dissolution of excess  $\text{TTA}^+$  from aggregated form to bulk aqueous solution. A schematic illustration of the lamella-to-micelle and micelle-to-vesicle transitions is shown in Figure 7.

Because the micelle-to-vesicle transition observed in other catanionic surfactant systems also occurs in nonequimolar mixtures, it is worth mentioning that they probably share the same mechanism as mentioned above. Thus, the mechanism of transitions shown in Figure 7 is also expected to work in other catanionic surfactant systems where the micelle-to-vesicle transition was also observed.<sup>36,37</sup> For charged aggregates with a fixed surfactant composition, the electrostatic repulsion between aggregates usually increases at higher temperature because of the dissociation of small counterions. However, the zeta potential was found to be almost constant at different temperatures in mixed system of SDS/dodecyltributylammonium bromide where SDS is in excess.<sup>56</sup> This is a proof of dissociation of SDS molecules into bulk aqueous solution with increasing temperature, which can lower the surface charge density of the aggregate and compensate for the opposite effect of small counterion dissociation.

(49) Vautrin, C.; Zemb, Th.; Schneider, M.; Tanaka, M. *J. Phys. Chem. B* **2004**, *108*, 7986.

(50) Israelachvili, J.; Mitchell, D. J.; Ninham, B. J. *J. Chem. Soc., Faraday Trans. 2* **1976**, *72*, 1525.

(51) Ninham, B. W.; Evans, D. F.; Wel, G. J. *J. Phys. Chem.* **1983**, *87*, 5020.

(52) Talmon, Y.; Evans, D. F.; Ninham, B. W. *Science* **1983**, *221*, 1047.

(53) Brady, J. E.; Evans, D. F.; Kachar, B.; Ninham, B. W. *J. Am. Chem. Soc.* **1984**, *106*, 4279.

(54) Majhi, P. R.; Blume, A. *J. Phys. Chem. B* **2002**, *106*, 10753.

(55) Egelhaaf, S. U.; Schurtenberger, P. *Phys. Rev. Lett.* **1999**, *82*, 2804.

(56) Yin, H.; Huang, J.; Gao, Y.; Fu, H. *Langmuir* **2005**, *21*, 2656.

## Conclusions

In summary, we have investigated the aggregate transitions in salt-free cationic surfactant mixtures as a function of surfactant concentration and temperature. Typically in the TTAOH/LA mixture with  $\rho = 0.88$ , two dominating aggregate transitions have been detected. With increasing temperature, an  $L_\alpha$ -to- $L_1$  phase transition via an intermediate  $L_\alpha/L_1$  two-phase region occurs at higher  $c_T$ , which corresponds to an aggregate transition from lamella (open bilayer) to micelle. At lower  $c_T$ , an  $L_1$ -to- $L_{\alpha'}$  phase transition is induced via an intermediate  $L_{\alpha'}/L_1$  two-phase region, which corresponds to an opposite aggregate transition from micelle to vesicle (closed bilayer). Although bilayer-to-micelle transition and micelle-to-bilayer transitions have been observed separately in other surfactant systems, they are seldom present in the same system. The TTAOH/LA mixture is shown to be a perfect model system for investigating these transitions, and this is the first system to exhibit both bilayer-to-micelle and micelle-to-bilayer transitions with increasing temperature. Similar aggregate transitions have been observed in the TTAOH/MA and TTAOH/PA mixtures. The replacement of LA by MA or PA, which have longer chain lengths than LA, induces a small difference. This includes a higher average Krafft point, a wider

$L_{\alpha'}$ , a phase-separated region, the absence of a single  $L_1$ -phase region, and a more pronounced  $L_{\alpha'}$ -to- $L_\alpha$  phase transition within the phase-separated region.

**Acknowledgment.** This work was supported by the project operated within the Foundation for Polish Science Team Programme cofinanced by the EU “European Regional Development Fund” TEAM/2008-2/2 and also by the Human Frontiers Science Program Organization and a MISTRZ grant from FNP. Dr. Hao is grateful for financial support by the NSFC (grant no. 20625307) and the National Basic Research Program of China (973 program, 2009CB930103). We are grateful to Prof. Garstecki for useful comments and discussions.

**Supporting Information Available:** Additional SAXS results on lamellar phases, fluorescence microscopy and polarized microscopy images, and evolution of the volume fraction of the upper  $L_\alpha$  phase as a function of surfactant concentration and temperature within the phase-separated region. This material is available free of charge via the Internet at <http://pubs.acs.org>.